

ON THE INVESTIGATION OF A RESTRAINED CARGO SYSTEM MODELED AS A DUFFING OSCILLATOR OF VARIOUS ORDERS

J. C. Lesage¹
Lakehead University
Thunder Bay, ON, Canada

M. L. Liu²
Lakehead University
Thunder Bay, ON, Canada

ABSTRACT

Many physical systems are inherently nonlinear. The nonlinear dynamic behavior of Duffing-type oscillators has long been an area of intensive research. A variety of methods are available for the analysis of Duffing-type oscillators whose nonlinearity and excitation can be weak or strong, and whose resonant frequency can be primary, or super-harmonic, or sub-harmonic. However, such research remains mostly the domain of mathematics or academics.

In this paper, the process and preliminary results of an investigation of the dynamic behavior of a cargo system under crossover indirect tiedown are presented. The cargo system is modeled as cubic, cubic-quintic and cubic-quintic-septic Duffing oscillators. The non-dimensional form of the equation of motion is derived and adopted for analysis. Free and forced oscillations are examined and the results are reported. The equations required for the jump frequency analysis, stability boundary analysis, and steady-state response analysis of a cubic-quintic-septic Duffing oscillator are derived. To the authors' knowledge, these are equations that have not been seen in the open literature.

It is found that a septic polynomial approximation of the nonlinear restoring force would be a prudent choice, which avoids the limitations associated with small nonlinearity and low level of excitation approximations. Lower-degree polynomials are sufficient for representing the restoring force itself, but are not adequate for the investigation and understanding of the dynamic behavior of the system. From the viewpoint of practical significance, the cargo system is found to have down-sweep jumps at a relatively low frequency. Such jumps can cause undue damage to the cargo.

1. INTRODUCTION

The nonlinear dynamic behavior of a Duffing-type oscillator has long been an area of intensive research. Many methodologies have been proposed for the nonlinear problem, from the classical approaches such as the straightforward expansion, the perturbation method, and the methods of multiple scales, harmonic balance and averaging [1], to analytical solutions for special cases (see, for example, Refs. [2, 3]) and other methods (for instance, the target function method [4], the high dimensional harmonic balance approach [5], and the extended averaged equation approach [6], to list just a few). These methods have enabled a rather wide range of analyses of the Duffing oscillator. Cases where the nonlinearity can be weak to strong, and where the periodic excitation causes primary, super-harmonic or sub-harmonic resonance have been investigated. Excitations such as periodic impulses [7] and stochastic forcing [8] have also been studied.

To the authors' best knowledge, research efforts have so far been more mathematically or academically oriented. Theoretical developments aside, almost all examples in the open literature make use of parameters that are easy to work with, such as integers and simple fractions. Unfortunately, in applications of practical interest, the relevant parameters are rarely so convenient.

In this article, an attempt by the authors to apply the established nonlinear dynamics analysis methodologies to an engineering system is presented. The article will outline the process and preliminary results of an investigation into the nonlinear dynamic behavior of a restrained cargo under crossover indirect tiedown. The emphasis of this research is not to develop a new method of nonlinear analysis; rather it is the judicious and effective application of existing methods to an engineering problem.

¹ Now at the Department of Mechanical Engineering, University of Toronto, Toronto, ON, Canada.

² Corresponding author.

The organization of the article is as follows. Section 2 deals with the equations of motion of the restrained cargo and its dimensionless form. It is also concerned with the representation of the nonlinear restoring force. Sections 3 and 4 present preliminary results for free- and forced oscillations, respectively. Finally, the article concludes with a summary.

2. THE RESTRAINED CARGO SYSTEM

Figure 1 shows the schematic of a restrained cargo secured by crossover indirect tiedown and its free-body diagram [9]. Where the mass of the cargo is m , the spring constant of the tiedown is k , tiedown angle is θ , initial length of the tiedown is L , initial tension in the tiedown is P_0 , and the coefficient of cargo-deck friction is μ_s . Longitudinal acceleration a_x is induced by braking. Vertical acceleration a_z is induced by the uneven surface over which the cargo is traveling. The longitudinal component of the restoring force is given by,

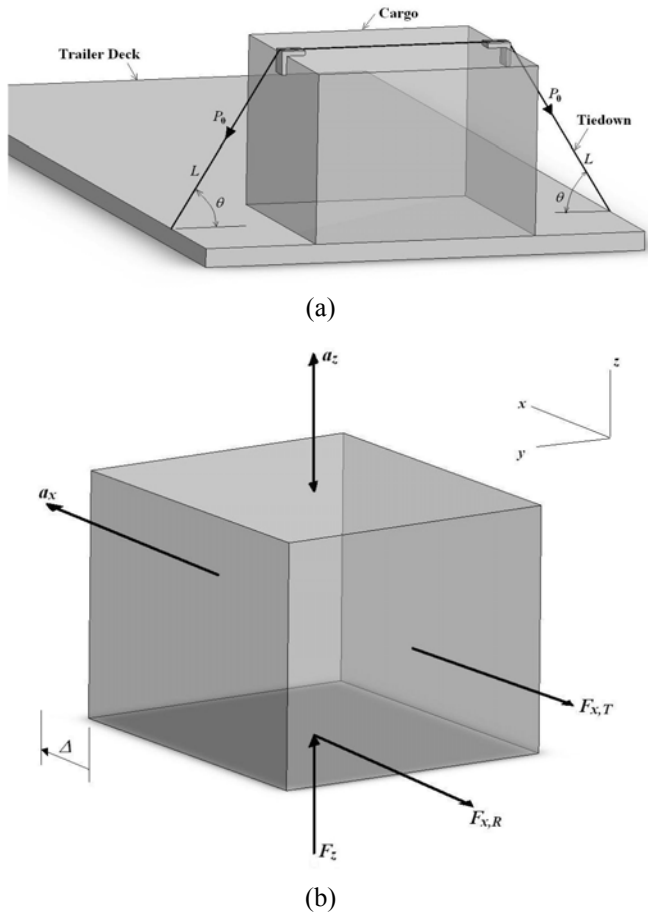


Figure 1. (a) Schematic and (b) Free-Body Diagram of a Restrained Cargo.

$$F_{x,T} = 2\Delta \left[k + \frac{P_0 - kL}{\sqrt{L^2 + \Delta^2}} \right] \quad (1)$$

where Δ is the longitudinal displacement of the cargo. The equivalent longitudinal stiffness of the tiedown is, with small Δ ,

$$\begin{aligned} k_E &= \frac{dF_{x,T}}{d\Delta} = 2 \left[k + \frac{L^2(P_0 - kL)}{(L^2 + \Delta^2)^{\frac{3}{2}}} \right] \\ &\approx 2 \left[k + \frac{P_0 - kL}{L} \right] \\ &= 2 \frac{P_0}{L} \end{aligned} \quad (2)$$

The friction force is,

$$\begin{aligned} F_{x,R} &= \mu_s F_z \\ &= 2\mu_s L \sin \theta \left(k + \frac{P_0 - kL}{\sqrt{L^2 + \Delta^2}} \right) \\ &\quad + \mu_s m (g + a_z) \end{aligned} \quad (3)$$

The equation of motion is therefore,

$$\begin{aligned} m \ddot{\Delta} &= -F_{x,T} - \text{sgn}(\dot{\Delta}) F_{x,R} - ma_x \\ &= -2 \left[k + \frac{P_0 - kL}{\sqrt{L^2 + \Delta^2}} \right] \Delta \\ &\quad - \text{sgn}(\dot{\Delta}) \left[2\mu_s L \sin \theta \left(k + \frac{P_0 - kL}{\sqrt{L^2 + \Delta^2}} \right) \right] \\ &\quad - \text{sgn}(\dot{\Delta}) [\mu_s m (g + a_z)] - ma_x \end{aligned} \quad (4)$$

where the double-dot indicates a second time-derivative, and “sgn” is the signum function. The right hand side, RHS, of Equation (4) is nonlinear in Δ . To represent it by simple polynomials, parametric studies are first conducted, taking into account the findings of Reference [9]. It is decided that the coefficient of friction would be set to zero at this preliminary phase. The reason is three-fold. Firstly, Reference [9] found that, without friction, the cargo displacement and tiedown tension both achieved their respective maximum values, a so-called “worst-case” scenario; secondly, the presence of friction would necessitate the inclusion of even degree (constant, second degree, etc.) terms in the polynomial, leading to a nonlinear system of non-Duffing type; and lastly, in the next phase, the friction will be re-introduced by the means of harmonic balance. Consequently the effect of vertical acceleration could not be considered, if strictly adhering to Equation (4). In Section 4, the cargo system will be examined for its un-damped forced-oscillation responses, although it would be ideal to consider damped forced oscillation.

The parametric studies show that, depending on the range of Δ , a cubic or a quintic polynomial provides a sufficient representation of the restoring force. Table 1 lists the coefficients of some of these polynomials. The following system parameters are used in obtaining the coefficients: $m = 100$ kg, $\theta = 45^\circ$, $L = 0.495$ m, $k = 3250$ kN/m and $P_0 = 0.5mg$ (N). In Table 1, Case I represents a relatively small range of Δ , hopefully corresponding to a small nonlinearity. The range of Δ for Case II is ten times that of Case I, hence a more strongly nonlinear situation.

Table 1. Polynomial Coefficients for Approximating Restoring Force

Case I: $\Delta = [-0.05, 0.05]$ (m)		
Cubic	Quintic	Septic
$R^2 = 0.99999^*$	$R^2 = 1.0000$	$R^2 = 1.0000$
$C_1 = 2.0440 \times 10^3$	$C_1 = 1.9821 \times 10^3$	$C_1 = 1.9819 \times 10^3$
$C_3 = 1.3147 \times 10^7$	$C_3 = 1.3261 \times 10^7$	$C_3 = 1.3261 \times 10^7$
	$C_5 = -4.0034 \times 10^7$	$C_5 = -4.0591 \times 10^7$
		$C_7 = 1.3546 \times 10^8$
Case II: $\Delta = [-0.5, 0.5]$ (m)		
Cubic	Quintic	Septic
$R^2 = 0.99$	$R^2 = 0.9999$	$R^2 = 0.99999$
$C_1 = 2.7814 \times 10^5$	$C_1 = 5.6916 \times 10^4$	$C_1 = 1.2674 \times 10^4$
$C_3 = 6.9578 \times 10^6$	$C_3 = 1.1009 \times 10^7$	$C_3 = 1.2574 \times 10^7$
	$C_5 = -1.4308 \times 10^7$	$C_5 = -2.7830 \times 10^7$
		$C_7 = 3.2871 \times 10^7$

* R^2 is the co-efficient of multiple determination.

At a first glance, it would seem that, for Case I a cubic polynomial would suffice, while Case II would require a quintic polynomial. It is noted that k_E is 2040.0 N/m from Equation (2). From Table 1, it can be seen that the values of C_1 for Case I are close to the value of k_E , indicating that Case I is indeed a small displacement case. Conversely, for Case II, none of the polynomials are able to capture the equivalent longitudinal stiffness. In fact, the C_1 values for Case II vary widely. A typical restoring force-displacement curve is given in Figure 2. The shape of the curve shows that the linear stiffness is small compared with the “higher-order stiffness”. For example, the cubic and quintic stiffnesses of Figure 2 are, 193 and 251 times, respectively, the linear counterpart. Note also the negative quintic stiffness.

Equation (4) can now be rewritten as,

$$m\ddot{\Delta} = - \sum_{j=1,3,5,7} C_j \Delta^j + A \cos \omega t \quad (5)$$

where without loss of generality, a septic polynomial is used to represent the restoring force. A sinusoidal

excitation has been added, where ω is the forcing frequency.

At this point it is appropriate to adopt the normalized form of Equation (5) by introducing the dimensionless time $\tau = \Omega t$, where $\Omega = \sqrt{\frac{C_1}{m}}$ is the natural frequency of the associated linear system. Dividing both sides of Equation (5) by C_1 , the dimension-less form of Equation (5) becomes,

$$x'' + x + k_3 x^3 + k_5 x^5 + k_7 x^7 = a \cos\left(\frac{\omega}{\Omega} \tau\right) \quad (6)$$

$$\approx a \cos(p\tau)$$

In Equation (6), it has been defined that $x(\tau) = \Delta(t) = \Delta\left(\frac{\tau}{\Omega}\right)$, and $k_3 = \frac{C_3}{C_1}$, $k_5 = \frac{C_5}{C_1}$, $k_7 = \frac{C_7}{C_1}$, $a = \frac{A}{C_1}$. The double prime denotes a second derivative with respect to τ . The quantity p represents the forcing frequency in the dimensionless time domain of τ .

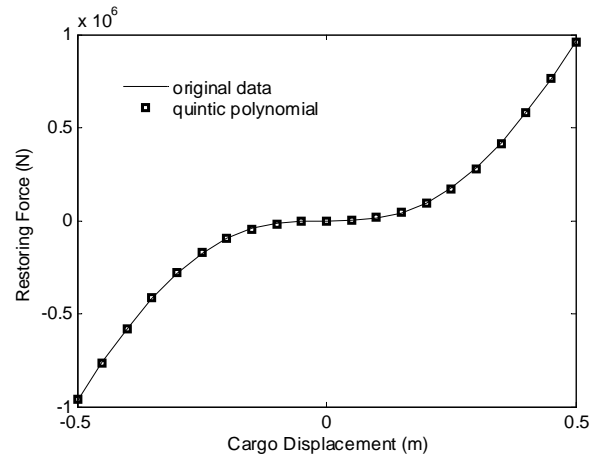


Figure 2. Restoring Force versus Displacement

3. THE UN-DAMPED FREE OSCILLATION

Typically the analysis of the un-damped free oscillation of a nonlinear oscillator involves the determination of the amplitude-dependent free-oscillation frequency, for which many solutions exist. Take the cubic Duffing oscillator as an example. Using the method of harmonic balance, Reference [1] gives, depending on the terms included in the assumed solution, $\bar{p} = \sqrt{1 + \frac{3}{4}k_3 X^2}$, or $\bar{p} = 1 + \frac{3k_3}{8} X^2$, or $\bar{p} = 1 + \frac{9k_3}{24} X^2$, where X is the amplitude of the steady-state free-oscillation, and \bar{p} is the frequency of free-oscillation in the dimensionless time domain. Since the nonlinearity in the cargo system is by no means weak, the higher-order approximate solutions proposed by Lai and Lim [10] are adopted. The first order approximate solution from [10] is the same as that given by the classical harmonic balance

method: $\bar{p}_{(1)} = \sqrt{1 + \frac{3}{4}k_3X^2}$ (where the subscripts “(1)” indicate first-order approximation). The second- and third-order solutions are much lengthier. For brevity, they are not repeated here. It should be noted that the solutions of [10] are for cubic Duffing oscillators only.

Table 2 lists some computed results of the amplitude-dependent free-oscillation frequencies. These results have been verified by the solutions by Wu *et al.* [11]. The two cubic Duffing oscillators from Table 1 are studied. The following is in order.

(1) The successive approximate solution of [10] yields upper solutions to the “true” frequency; the convergence pattern seems to be monotonic and from above; and

(2) If frequencies are to be accurate to the first decimal place, the first-order approximation is sufficient for all $X < \Delta_u$, where Δ_u is the range of Δ . On the other hand, if the accuracy is raised to, say, the third decimal place, the first-order approximation is only sufficient for $X = 0.05$ and 0.1 from Case II. In other words, the amplitude of oscillation is merely up to 25% of the range of displacement that the polynomial representation is intended for.

In summary, to evaluate the free-oscillation frequency accurately, one needs to, increase the range of Δ and the order of polynomial, or increase order of approximation. Finally, frequencies in the time domain, $\bar{\omega}_{(i)}$, can be determined via the relation $\bar{\omega}_{(i)} = \bar{p}_{(i)}\Omega$.

Table 2. Amplitude-Dependent Free-Oscillation Frequencies

Case I			
X (m)	$\bar{p}_{(1)}$	$\bar{p}_{(2)}$	$\bar{p}_{(3)}$
0.01	1.21754	1.21480	1.21459
0.025	2.00376	1.97857	1.96684
0.05	3.61389	3.54911	3.40702
Case II			
X (m)	$\bar{p}_{(1)}$	$\bar{p}_{(2)}$	$\bar{p}_{(3)}$
0.05	1.02318	1.02314	1.02314
0.1	1.08978	1.08921	1.08921
0.25	1.47397	1.46500	1.46493
0.5	2.38544	2.35143	2.35080

4. THE UN-DAMPED FORCED OSCILLATION

For forced oscillation analysis of a nonlinear oscillator, the steady-state response, or the amplitude versus frequency curves, will be sought, and the stability boundaries, in the frequency-amplitude plane, will be determined. Here the frequency refers to the frequency of excitation. The curves and boundaries will provide us

with information regarding the dynamic behavior of the oscillator. For instance, a jump frequency will tell us at what frequency the multi-valued-ness of the oscillation will begin or end. The boundaries will map where solutions are stable or unstable.

Similar to the free oscillation analysis, the method of analysis will be dictated by the strength of nonlinearity. In particular, Peng, *et al.* [12] stated that the harmonic balance method, when used with sufficient number of harmonics, would be an adequate tool for the analysis of strongly nonlinear systems. The drawback is that the method is not easy to implement, and is highly problem-dependent, in other words, the method is highly nonlinearity-dependent. Since $\cos^n(\omega t)$, when expanded, includes the n -th harmonic $\cos(n\omega t)$, the present investigation chooses to increase the degree of the polynomial in lieu of including higher harmonics.

Now considering the cubic-quintic-septic Duffing oscillator described by Equation (6), the assumed steady-state response takes the form of

$$x(\tau) = X \cos(p\tau) \quad (7)$$

Substituting Equation (7) into Equation (6), neglecting higher harmonics and simplifying lead to the following septic equation in terms of $Y = X^2$ [13]:

$$f_7Y^7 + f_6Y^6 + f_5Y^5 + f_4Y^4 + f_3Y^3 + f_2Y^2 + f_1Y + f_0 = 0 \quad (8)$$

where

$$\begin{aligned} f_7 &= \frac{1225}{4096}k_7^2, & f_6 &= \frac{175}{256}k_3k_7, \\ f_5 &= \frac{25}{64}k_5^2 + \frac{105}{128}k_3k_7, \\ f_4 &= \frac{15}{16}k_3k_5 + \frac{35}{32}k_7(1-p^2), \\ f_3 &= \frac{9}{16}k_3^2 + \frac{5}{4}k_5(1-p^2), \\ f_2 &= \frac{3}{2}k_3(1-p^2), & f_1 &= (1-p^2)^2, \\ f_0 &= -a^2. \end{aligned} \quad (9)$$

For a given p , multiple roots are found from Equation (8). Values for X are found by taking the square root of each root. Only the real X 's are retained, since an imaginary X has no physical meaning. Plots of X versus p give the amplitude versus frequency curves. It should be pointed out that Equations (8) and (9) have not been reported in the open literature, to the authors' knowledge.

For the stability of a steady-state response, the present investigation employs the classical approach of superposing a perturbation on a solved steady-state response. That is, the solution to Equation (6) is assumed the following form:

$$x(\tau) = X \cos(p\tau) + b(\tau) \quad (10)$$

where $b(\tau)$ is the perturbation and X has been determined from Equation (8). Substituting Equation (10) into Equation (6), the equation of motion of the cubic-quintic-septic Duffing oscillator, it is found that the perturbation $b(\tau)$ must satisfy the following condition [13]:

$$b'' + (c_1 + c_2 \cos 2p\tau)b \approx 0 \quad (11)$$

In Equation (11), only the first-order terms pertaining to the perturbation b are retained. The RHS of Equation (11) consists of higher harmonics, which are hence neglected. The quantities c_1 and c_2 are

$$\begin{aligned} c_1 &= 1 + \frac{3}{2}k_3a^2 + \frac{15}{8}k_5a^4 + \frac{35}{16}k_7a^6, \\ c_2 &= a^2 \left(\frac{3}{2}k_3 + \frac{5}{2}k_5a^2 + \frac{105}{32}k_7a^4 \right). \end{aligned} \quad (12)$$

Subsequently, it is assumed that

$$b(\tau) = u(\tau) \cos p\tau + v(\tau) \sin p\tau \quad (13)$$

Further, $u(\tau)$ and $v(\tau)$ are assumed to be slowly-varying such that their second derivatives with respect to τ are approximately zero. As a result, their respective first dimensionless time derivatives are [13]

$$\begin{aligned} -2pv' &= -p^2u + \frac{2c_1 + c_2}{2}u \\ 2pu' &= -p^2v + \frac{2c_1 - c_2}{2}v \end{aligned} \quad (14)$$

Writing Equation (14) in the matrix notation,

$$\begin{Bmatrix} u' \\ v' \end{Bmatrix} = \frac{1}{2p} \begin{bmatrix} 0 & -p^2 + \frac{2c_1 - c_2}{2} \\ p^2 - \frac{2c_1 + c_2}{2} & 0 \end{bmatrix} \begin{Bmatrix} u \\ v \end{Bmatrix} \quad (15)$$

The Jacobian matrix in Equation (15) has a zero trace and a determinant given by the following

$$\begin{aligned} \det &= \left(p^2 - \frac{2c_1 + c_2}{2} \right) \left(p^2 - \frac{2c_1 - c_2}{2} \right) \\ &= \left(p^4 - 2c_1p^2 + \frac{4c_1^2 - c_2^2}{4} \right) \end{aligned} \quad (16)$$

Therefore, if $\det \geq 0$, the steady-state response will be a stable center; otherwise, it will be a saddle point. Expanding the RHS of Equation (16) gives rise to the following condition for a stable steady-state solution [13]:

$$\begin{aligned} &\left(\frac{8575}{4096}k_7^2 \right) a^{12} + \left(\frac{525}{128}k_5k_7 \right) a^{10} + \\ &\quad + \left(\frac{125}{64}k_5^2 + \frac{525}{128}k_3k_7 \right) a^8 + \\ &\quad + \left[\frac{15}{4}k_3k_5 + \frac{35}{8}k_7(1 - p^2) \right] a^6 + \\ &\quad + \left[\frac{27}{16}k_3^2 + \frac{15}{4}k_5(1 - p^2) \right] a^4 + \\ &\quad + 3k_3(1 - p^2)a^2 + (1 - p^2)^2 = 0 \end{aligned} \quad (17)$$

Finally, jump frequencies are found by evaluating the roots of the equation obtained when the discriminant D of the left hand side (LHS) of Equation (8) is set equal to zero. This discriminant can be determined by first setting up the 13 by 13 Sylvester matrix R :

$$R = \begin{bmatrix} f_7 & f_6 & f_5 & \dots & f_1 & f_0 & 0 & \dots & \dots & 0 \\ 0 & f_7 & f_6 & f_5 & \dots & f_1 & f_0 & 0 & \dots & 0 \\ \vdots & & & & & & & & & \vdots \\ 0 & \dots & 0 & f_7 & f_6 & f_5 & \dots & \dots & f_1 & f_0 \\ 7f_7 & 6f_6 & 5f_5 & \dots & 1f_1 & 0 & \dots & \dots & \dots & 0 \\ 0 & 7f_7 & 6f_6 & 5f_5 & \dots & 1f_1 & 0 & \dots & \dots & 0 \\ \vdots & & & & & & & & & \vdots \\ 0 & 0 & 0 & 0 & 0 & 7f_7 & 6f_6 & \dots & 2f_2 & 1f_1 \end{bmatrix} \quad (18)$$

The discriminant D is then given by:

$$D = (-1)^{21} \frac{1}{f_7} \det(R) = -\frac{\det(R)}{f_7} \quad (19)$$

In passing, it is noted that Eqs. (11), (12) and (17) have not been seen in the open literature.

The computed jump frequencies are given in Table 3. Both Cases I and II are examined, each subjected to two levels of excitation. Since the oscillator is free of damping, one jump frequency is expected from the cubic Duffing model. The number of jump frequencies for the cubic-quintic and cubic-quintic-septic Duffing oscillators depend on the values of the stiffness terms. It is seen that, the cubic Duffing oscillator yields only one jump frequency. The cubic-quintic-septic model also gives one such frequency. The cubic-quintic Duffing oscillator has three real roots. Their physical significance will be identified later upon examination of the steady-state response, i.e. the amplitude versus frequency curves.

For steady-state response analysis, Case II is chosen with excitation level of $A = 1mg$. Results are presented in Figures 3 through 5. The following is in order.

Table 3. Computed Jump Frequencies

Case I, $A = 0.1mg$			
Degree of polynomial	1 st real root	2 nd real root	3 rd real root
cubic	2.2841	---	---
quintic	2.3152	22.3494	22.3543
septic	2.3153	---	---
Case I, $A = 1mg$			
Degree of polynomial	1 st real root	2 nd real root	3 rd real root
cubic	4.5359	---	---
quintic	4.6066	22.3270	22.3767
septic	4.6068	---	---
Case II, $A = 0.1mg$			
Degree of polynomial	1 st real root	2 nd real root	3 rd real root
cubic	1.0125	---	---
quintic	1.0690	5.8724	5.8729
septic	1.2930	---	---
Case II, $A = 1mg$			
Degree of polynomial	1 st real root	2 nd real root	3 rd real root
cubic	1.0566	---	---
quintic	1.2893	5.8705	5.8748
septic	2.0288	---	---

* --- means that a real root is not available.

(1) The single jump frequency in the cubic model is the down-sweep jump frequency (Figure 3). The up-sweep jump frequency does not exist due to zero damping. The regions of stable and unstable responses are correctly identified, comparing with published results in the literature. Note that for $p > 1.5$ (approx.), the centers and saddle points are indiscernible, although they are separated by a stability boundary.

(2) The frequency-amplitude plane of the cubic-quintic oscillator is divided into two regions of stable solutions, as well as two regions of unstable solutions (Figure 4). The cubic, and cubic-quintic-septic oscillators have only one unstable region (Figures 3 and 5).

(3) The lowest real root from the jump frequency analysis of the cubic-quintic oscillator corresponds to a down-sweep jump frequency (Figure 4). The two larger real roots, 5.8705 and 5.8748, are associated with the frequencies at which the stable centers (at 5.8748) and saddle points (at 5.8705) “bend backward”, see Figure 6 for a windowed view. Therefore, both are the up-sweep jump frequencies. The backward bend is due to the negative-ness of the quintic stiffness, as opposed to the positive cubic and septic stiffnesses.

(4) For the cubic-quintic-septic model, the only real root found from jump frequency analysis is seen to be the down-sweep jump frequency (Figure 5).

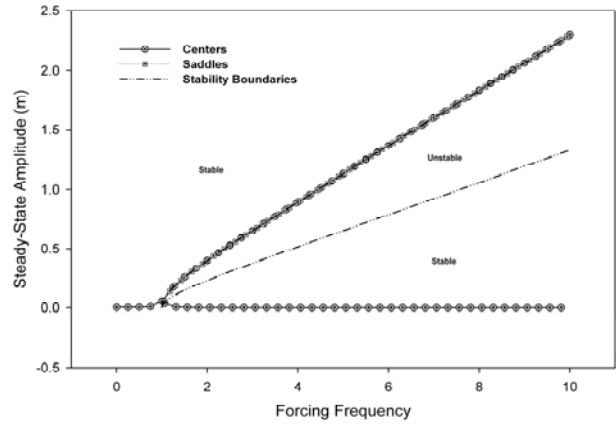


Figure 3. Response and Stability Boundary [Cubic Duffing, Case II]

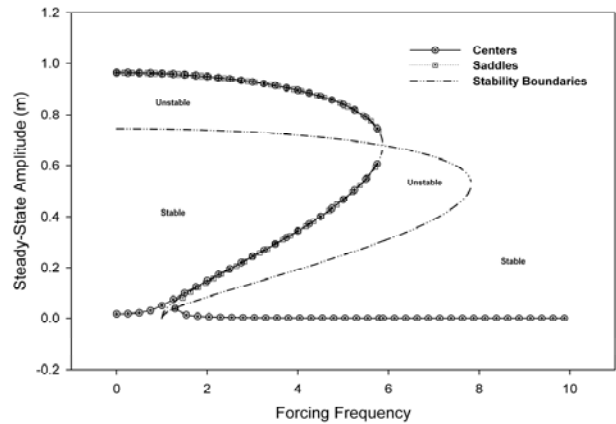


Figure 4. Response and Stability Boundary [Cubic-Quintic Duffing, Case II]

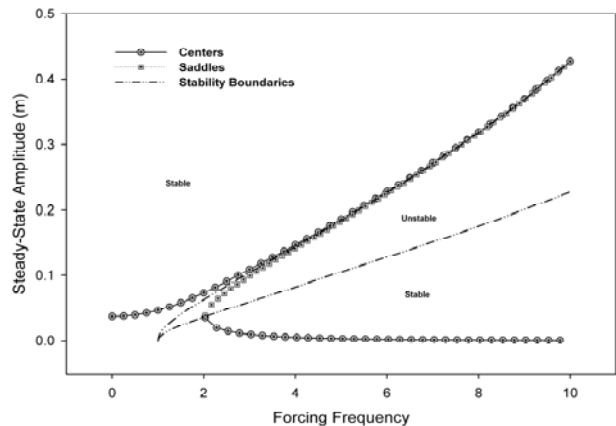


Figure 5. Response and Stability Boundary [Cubic-Quintic-Septic Duffing, Case II]

(5) In terms of the overall dynamic behavior, the cubic-quintic Duffing oscillator provides more insight into the dynamic behavior of the system. For example, it has the two up-sweep jumps and an extra unstable region. At the frequency range of $0 \sim 5.87$ (approx.), the oscillator also possesses a steady-state solution that is of higher amplitude ($0.7 \sim 0.98$, approx.). If one is to focus on the low-frequency-and-low-amplitude window (Figure 7), the oscillators are seen to be similar to each other, qualitatively speaking. The differences in the positioning of the backbone, the location of the down-sweep jump, and the range of the resulting steady-state amplitude are due to the wide range of C_1 values, see Table 1 and the discussions following it.

(6) Equally important is the observation that, at and around the down-sweep jump frequency, the upper steady-state amplitude is greater than 0.05 m. This means that the small displacement case is unrealistic. Furthermore, this implies that the cubic approximation should be used with care. Such an approximation is adequate only if the nonlinearity is *indeed* small. Since in real world applications the strength of nonlinearity is usually guess work at best, employing the cubic-quintic-septic Duffing would prove prudent. The latter removes such restrictions as weak nonlinearity and excitation. Its steady-state response does not show the physically unlikely higher-amplitude solution, or the backward bend. Therefore, the cubic-quintic-septic Duffing oscillator seems to represent the physical system with sufficient accuracy.

5. CONCLUSIONS

In this article, the process and preliminary results of an investigation into the dynamic behavior of a cargo system under crossover indirect tiedown are outlined. The cargo system is modeled as cubic, cubic-quintic and cubic-quintic-septic Duffing oscillators. The non-dimensional form of the equation of motion is derived and adopted for analysis. Free and forced oscillations are examined and the results are reported. The equations required for the jump frequency analysis, stability boundary analysis, and steady-state response analysis of a cubic-quintic-septic Duffing oscillator are derived. To the authors' knowledge, these equations have not been reported in the open literature.

With regard to the modeling of the cargo system, although the cubic and cubic-quintic representations were found to adequately represent the restoring force itself, it is suggested that the cubic-quintic-septic approximation of the nonlinear restoring force would be used for the investigation of the dynamic behavior of the system. Using the cubic-quintic-septic oscillator model avoids limitations associated with approximations such as small

nonlinearity and low level of excitation, and is found to represent the physical system sufficient accuracy.

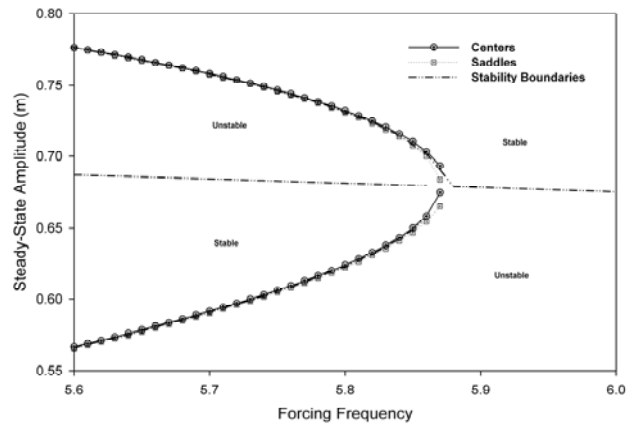


Figure 6. Windowed View of the Cubic-Quintic Oscillator, Case II

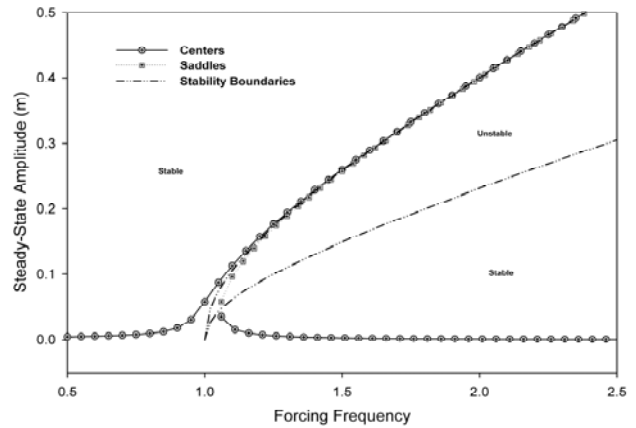


Figure 7(a)

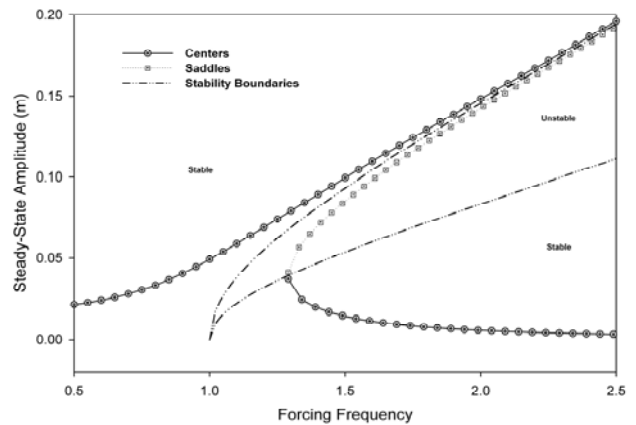


Figure 7(b)

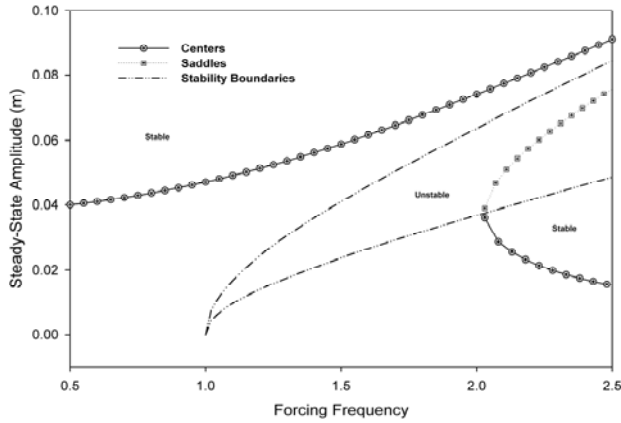


Figure 7(c)

Figure 7. Comparison of the Duffing Oscillators.
(a) Cubic; (b) Cubic-Quintic; and (c) Cubic-Quintic-Septic.

From the viewpoint of practical significance, the cargo system is found to have a down-sweep jump at a relatively low frequency. Such a jump would be encountered when the vehicle carrying the cargo is reducing its speed and could cause undue damage to the cargo.

ACKNOWLEDGMENT

The work reported in this article was performed during the summer of 2007. The first author gratefully acknowledges the USRA (Undergraduate Summer Research Award) that was awarded to him by NSERC (Natural Sciences and Engineering Research Council of Canada). The second author is grateful for the financial support provided by NSERC through a Discovery Grant.

REFERENCES

[1] Nayfeh, A. H., and Mook, D. T., 1979, *Nonlinear Oscillations*, John Wiley & Sons, N.Y., U.S.A., Chaps. 2-3.

[2] Chen, S.H., and Cheung, Y. K., 1996, "An Elliptical Perturbation Method for Certain Strongly Nonlinear Oscillators," *J. Sound Vib.*, 192(2), pp. 453-464.

[3] Roy, R. V., 1994, "Averaging Method for Strongly Nonlinear Oscillators with Periodic Excitations," *Int. J. Non-Linear Mech.*, 29(5), pp. 737-753.

[4] Chen, Y. Z., 2002, "Solution of the Duffing Equation by Using Target Function Method," *J. Sound Vib.*, 256(3), pp. 573-578.

[5] Liu, L., Thomas, J. P., Dowell, E. H., Attar, P., and Hall, K. C., 2006, "A Comparison of Classical and High Dimensional Harmonic Balance Approaches for a Duffing Oscillator," *J. Computational Phys.*, 215, pp. 298-320.

[6] Anh, N. D., Hai, N. Q., and Schiehlen, W., 2007, "Nonlinear Vibration Analysis by an Extended Averaged Equation Approach," *Nonlinear Dyn.*, 47, pp. 235-248.

[7] Bapat, C. N., 1995, "Duffing Oscillator under Periodic Impulses," *J. Sound Vib.*, 179(4), pp. 725-732.

[8] Datta, S., and Bhattacharjee, J. K., 2001, "Effect of Stochastic Forcing on the Duffing Oscillator," *Phys. Lett. A.*, 283, pp. 323-326.

[9] Romero, J. A., Rakheja, S., Ahmed, A. K. W., and Lozano, A., 2002, "Restrained Cargo Dynamics in Road Transportation Indirect Tiedowns," *Heavy Veh. Syst.* 9(2), pp. 93-114.

[10] Lai, S. K., and Lim, C. W., 2006, "Higher-Order Approximate Solutions to a Strongly Nonlinear Duffing Oscillator," *Int. J. Computational Methods Engineering Science & Mechanics*, 7, pp. 201-208.

[11] Wu, B. S., Sun, W. P., and Lim, C. W., 2006, "An Analytical Approximate Technique for a Class of Strongly Nonlinear Oscillators," *Int. J. Non-Linear Mech.*, 41, pp. 766-774.

[12] Peng, Z. K., Lang, Z. Q., Billings, S. A., and Tomlinson, G. R., 2008, "Comparisons between Harmonic Balance and Nonlinear Output Frequency Response Function in Nonlinear System Analysis," *J. Sound Vib.*, 311, pp. 56-73.

[13] Lesage, J. C., and Liu, M. L., 2007, "Summary of Cargo System Dynamics Research," Technical Report, Department of Mechanical Engineering, Lakehead University, Thunder Bay, ON, Canada.